Kufa Journal of Engineering
Vol. 16, No. 1, January 2025, P.P. 177-199
Article history: Received 8 June 2024, last revised 9 August 2024, accepted 9 August 2024

INVESTIGATION OF FREE VIBRATION BEHAVIOR FOR COMPOSITE SANDWICH BEAMS WITH A COMPOSITE HONEYCOMB CORE

Zainab Majid Jasim[1] and Husam Jawad Abdulsamad [2]

[1] Engineer, University Of Kufa, College Of Engineering, Department Of Mechanical Engineering, Najaf, Iraq, Email: zainabm.altameemi@student.uokufa.edu.iq.

[2] Assistant Professor, University Of Kufa, College Of Engineering, Department Of Mechanical Engineering, Najaf, Iraq, Email: Husamj.alhamad@uokufa.edu.iq.

https://doi.org/10.30572/2018/KJE/160111

ABSTRACT

The purpose of the current research is to determine the effect of fiber type, volume ratio, and matrix type on the vibration properties of sandwich beams made of composite face sheet and core. The typical sandwich structure consists of three layers: face sheets, core, and adhesive bonding, and in this research, the adhesive layer between the face sheets and core was abolished by preparing the overall mold with fibers inside and casting the resin to fill the face sheet and core parts. The face sheets of the composite beams are made from a polyester or epoxy matrix reinforced with glass fiber, carbon fiber, and hybrid fiber, and the core is a honeycomb consisting of random glass fibers immersed in a resin matrix (polyester or epoxy). 22 composite sandwich beams were constructed to conduct vibration testing. The vibration results obtained experimentally were compared to the ANSYS R1 2022 software, and the results were in very good agreement. Hybrid fibers and polyester matrix achieved the highest values of natural frequency for (clamped-clamped) boundary conditions, where the natural frequency value of the hybrid fiber and polyester matrix reached (2037 Hz) at a volume fraction of (23.14%) experimentally and the natural frequency reached (1804.5 Hz) at a volume fraction of (21.95%) experimentally for the simply supported boundary condition.

KEYWORDS

Sandwich beams, Vibration test, ANSYS R1 2022, Hybrid fibers, Honeycomb core.

1. INTRODUCTION

Composite sandwich structures have received a lot of attention. The composite structure has unique mechanical properties, including a high strength-to-weight ratio and excellent energy absorption. Because of these mechanical properties, the composite material outperforms many other materials in a variety of applications. Several studies were performed in the field of composite sandwich beams that will be discussed through three classifications: metal composite sandwich beams, polymer composite sandwich beams, and FGM composite sandwich beams. (Monti, El Mahi et al. 2017) investigated the flexural vibration behavior of bio-based sandwich constructions and their composite faces. They found that the damping factor appears to be highest for low frequencies in all laminates; also, the skin's Young's modulus and loss factor, as well as the core's shear modulus and loss factor, were regarded as frequency dependent. (De Souza Eloy, Gomes et al. 2018) discovered that by using a magnetic field of varying intensity for free and forced vibration testing on MRE sandwich beams made of carbon fiber/epoxy skins and 3D printed honeycomb cores, it is possible to reduce the natural frequency. (Subramani, Rajeshkumar et al. 2020; Selvaraj and Ramamoorthy 2021; Selvaraj, Ramamoorthy et al. 2021) investigated the free vibration response of sandwich beams consisting of polymer composite skins and multiwalled carbon nanotubes. It was concluded that the presence of multiwall carbon nanotubes (MWCNTs) significantly influences the vibration behavior of sandwich structures. (Ebrahimi and Farazmandnia 2017; Ebrahimi and Farazmandnia 2018;Ebrahimi, Farazmandnia et al. 2018; Marandi and Karimipour 2023; Momeni, Dehkordi et al. 2019; Ebrahimi, Farazmandnia et al. 2017) investigated the free vibration analysis of functionally graded carbon nanotube-reinforced composite (FG-CNTRC) sandwich beams using different theories. They concluded that the (FG-CNT) reinforcement in the face sheets contributed to increased stiffness, strength, and thermal stability of the sandwich beams, leading to improved structural performance. (Nguyen, Vu et al. 2020) utilized a numerical investigation to examine the dynamic response of the bidirectional functionally graded sandwich (BFGSW) beam under nonuniform motion of a moving load. Results show that the dynamic behavior of this beam is significantly influenced by the acceleration and deceleration of the moving load, the material distribution, and the layer thickness ratio. (Liu, Lv et al. 2019) found that the influence of initial geometric imperfection on the nonlinear vibration behavior of functionally graded (FG) sandwich nanobeams in the presence of initial geometric imperfection may depend on the specific type of nanobeam being considered. (Liu, Hao et al. 2021) found that The scaled boundary finite element method (SBFEM) offers advantages in reducing spatial dimensions and time-consuming processes and thus addressing the challenges associated with dynamic analysis of free and forced vibrations of (FGM) sandwich beams. (Yildirim 2020) studied the vibration behavior of a sandwich thermal protection system insulation panel with a functionally graded core using the complementary functions method. The method demonstrated its accuracy and efficiency in the thickness direction. (Bakhy, Al-Waily et al. 2021), conducted an analytical and numerical investigation of the free vibration of functionally graded materials (FGMs) sandwich beams. It was concluded, that the increase in the number of layers prompts an increment within the frequency parameter results' accuracy for the selected models. (Aslan, Noori et al. 2023), found that The complementary functions method can be implemented easily and efficiently to handle free vibration response of FG sandwich beams of variable cross-section. (Selvaraj, Subramani et al. 2021; Selvaraj, Gupta et al. 2021 and Thanikasalam and Ramamoorthy 2023) founds that the double and multi -cores composite beams exhibit higher stiffness and better dynamic behavior compared to single-core composite beam through using both experimental and numerical methods to investigate the vibration responses. (Gopalan, Suthenthiraveerappa et al. 2020), found that specific combinations of core thickness, number of layers, and fiber angle orientation significantly impact the natural frequencies and mode shapes of the sandwich beam. (Liu, Yang et al. 2021), found that multi-span sandwich beams with pyramidal truss core exhibit better vibration and thermal buckling stability when the sub span lengths are adjusted, and the number of sub spans is increased. (Alambeigi, Mohammadimehr et al. 2020), concluded that the vibration behavior of a sandwich beam resting on an elastic foundation which is simulated by Vlasov's model with functionally graded porous core and composite face layers reinforced with carbon nanotubes (CNT) embedded with shape memory alloy (SMA) is significantly influenced by parameters such as SMA wires, porosity, and temperature. (Nematollahi, Mohammadi et al. 2020) found that the sensitivity of the nonlinear vibration behavior of thick sandwich nanocomposite beams reinforced by functionally graded (FG) graphene nanoplatelet (GPL) sheets, with a power-law-based distribution throughout the thickness varies with the total amount of GPL reinforcement in the beam, the value of the power-law parameter and the thickness of the face sheets. (Chen, Kitipornchai et al. 2016) concluded that an increase in the vibration amplitude leads to a larger nonlinear frequency ratio of shear deformable sandwich porous beam using Timoshenko beam theory of nonlinear free vibration behavior. (Xin and Kiani 2023), demonstrated that the porosity of the core for any thickness sandwich beam with a functionally graded metal foam core is to be a key influence in the vibration characteristics and the addition of an elastic basis to a metal foam sandwich beam raises the inherent frequencies. (Elmushyakhi 2019), determined the conditions that lead to catastrophic failure. It's found that Preloading beams at

70% in various composite sandwich construction materials causes delamination to begin quickly, also Matrix-cracking began at 60% preloading. (Gopalan, Suthenthiraveerappa et al. 2020), found that the optimum dynamic characteristics of sandwich beam built of polypropylene honeycomb as the core and a woven jute/epoxy laminated composite as the face sheet are obtained from specimens with a core thickness of (10 mm) or less, a layer count of two to three, and a fiber angle orientation of around 20°. (Taati and Fallah 2019), investigated the frequency response of clamped and simply supported microbeams with functionally graded (FG) cores. It's found that the frequency behavior of clamped microbeams is dependent on essential and natural size-dependent boundary conditions, contrary to beams with simple supports. (Erdurcan and Cunedioğlu 2020), examined the free vibration of a symmetric beam made up of an aluminum core coated with functionally graded material theoretically. The analyzed characteristics were shown to have a considerable effect on the natural frequencies. (Bakhy, Al-Waily et al. 2021), found that increasing the number of layers of FG sandwich beams composed of functionally graded core and face sheets made of an isotropic uniform material causes an increase in the frequency parameter's accuracy for the Euler-Bernoulli beam theory and the Finite element method used in the search. (Avcar, Hadji et al. 2021), used high-order shear deformation theory to investigate the natural frequencies of sigmoid functionally graded (FG) sandwich beams of various configurations. Its concluded that the skin-core-skin thickness ratio and the shear deformation hypothesis and the increase in mode number influence non-dimensional natural frequencies. (Liu, Hao et al. 2021), compared between the results of the scaled boundary finite element method (SBFEM) for examine free and forced vibrations of functionally graded material (FGM) sandwich beams and the results produced using different theories in the other literature, and there is good agreement. (Safaei, Onyibo et al. 2023), evaluated the stress state, modal, and free vibration studies of honeycomb sandwich constructions with various boundary conditions. It was concluded that fatigue resistance, resonance, and deformation resistance can all be improved at higher frequencies by adding a reinforced star-shaped core. (Li, Wang et al. 2024), examined how sandwich constructions with auxetic honeycomb cores behaved during thermally induced vibration (TIV) experiments using various thermal shocks. They demonstrated that, in comparison to linear theory, geometric nonlinearity can result in variations in the frequency and amplitude of TIV responses, especially under various thermal shock scenarios. (Lu, Wang et al. 2022), showed that the suggested novel adaptive closed-loop control system for composite sandwich beams successfully reduce low-frequency vibrations. (Chen and Su 2021), provided an analytical solution based on the refined zigzag theory (RZT) for vibration in cantilevered functionally graded (FG) sandwich beams. The RZT is shown to be highly suitable for determining the mode shapes, natural frequencies, and frequency responses of FG sandwich beams.

The aim of this work is to investigate the effect of different types of fibers with two types of matrix materials on the vibration performance represented by the natural frequency for composite sandwich beams with composite honeycomb core.

2. THE MECHANICAL PROPERTIES OF THE USED MATERIALS

The specifications of the materials used are summarized in Tables (1 - 5) as follows:

Table 1: The mechanical properties of E-glass

Density (kg/m^3)	Tensile strength (GPa)	Modulus of elasticity E (GPa)	Shear Modulus G (GPa)	Poisson Ratio ν
2600	2.5	74	30	0.25

Table 2: The mechanical characteristics of woven glass fiber

Density (g/cm^3)	Sizing content (%)	Thickness (mm)	Tensile strength at break (N/5cm)		Poisson ratio
2.6	0.5~2.0	0.22	warp ≥5500	weft ≥5000	0.21

Table 3: The mechanical characteristics of carbon fibers

Density(g/cm3)	Tensile Strength Mpa	Thickness(mm)	Poisson ratio
1.8	≥3400	0.167	0.2

Table 4: Mechanical properties of epoxy matrix

Density ($\frac{Kg}{m^3}$)	Poisson ratio	Young Modulus (GPa)
1100	0.3	1.9

Table 5: The mechanical properties of polyester matrix

Density ($\frac{\mathrm{Kg}}{\mathrm{m}^3}$)	Modulus of elasticity E (GPa)	Tensile strength (GPa)	Elongation (%)	Viscosity (cps)
1130	3	0.05	2.5	575– 675

Table 1 represents the mechanical properties of E-glass fibers. The mechanical properties of woven glass fiber are shown in Table 2 in accordance with the product data sheet /F. T. C. L./ China. Carbon fibers' mechanical properties are shown in Table 3 based on the product data sheet/H. A. C. M. C. L. The mechanical characteristics of the epoxy matrix were displayed in Table 4 in accordance with the N. T. 2021 Data sheet of Epoxy resin (Renksan - Renfloor HT 2000)/USA. Additionally, Table 5 shows the polyester matrix's mechanical characteristics based on the "Technical Data Sheet" from Saudi Industrial Resins Limited in Dammam.

3. FABRICATION PROCESS OF SANDWICH BEAM TEST SPECIMEN

The following steps are required to cast the specimens:

1. Glass spacers are installed on one face of each of two plates of glass and on both longitudinal edges.

2. Two pieces of glass are brought between the two primary mold plates.
3. The parts of the mold are connected using glue. Then the glue is waited to dry and the parts to bond completely.
4. The glass plates are painted with a thin layer of wax to prevent the fibers from sticking to the resin.
5. The required glass fiber fabric is cut into the necessary dimensions and placed on each side of the mold.
6. A hexagonal section pen and a half hexagonal pen are used to create the hexagonal holes of the honeycomb core.
7. Three layers of random glass fiber fabric were cut and sewn together successively with insertion of the hexagonal section pen between the three layers to form the honeycomb setting.
8. The honeycomb setting is placed and centered between the two sides of the mold, with the half-hexagonal pens positioned at the top and bottom. A space of two centimeters is left empty without a core from both sides, as shown in Fig.1.

Fig. 1. Placing the half hexagonal pens on the other side of the core

9. The mold base is bonded to the side parts of the mold using the glue.
10. The mold is installed using two clamps (one clamp on each side), see Fig.2.

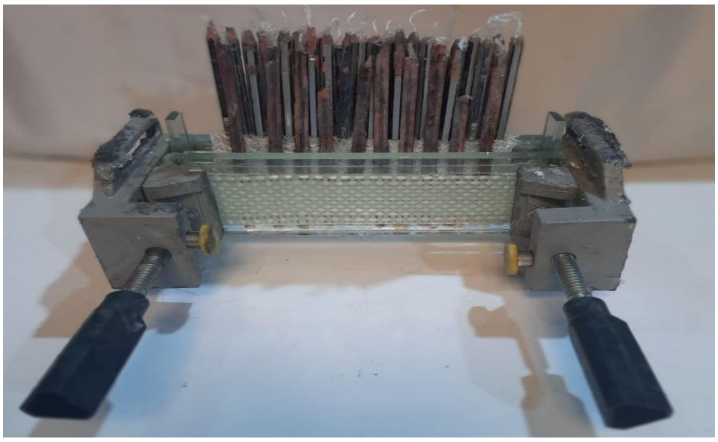

Fig.2. Installing and fixing the mold parts using the clamps

11. The glue should be left to dry for an hour to prevent resin leakage.
12. The required resin (polyester or epoxy) is prepared and poured from both the left and right empty sides of the mold until it is filled. The resin flows from the mold base to the mold top through the fibers, fills the spaces between the fibers, and ousts the air. This prevents the formation of voids. The casting process is done in room-temperature environments.
13. The pens are withdrawn when the required resin reaches the gelatin stage.
14. After withdrawing the pens, wait until the specimen dries completely, then open the mold and extract the specimen.

The sandwich beam specimens were finished using the slide cutting saw machine, according to (ASTM C393-00 standard) as shown in Fig.3.

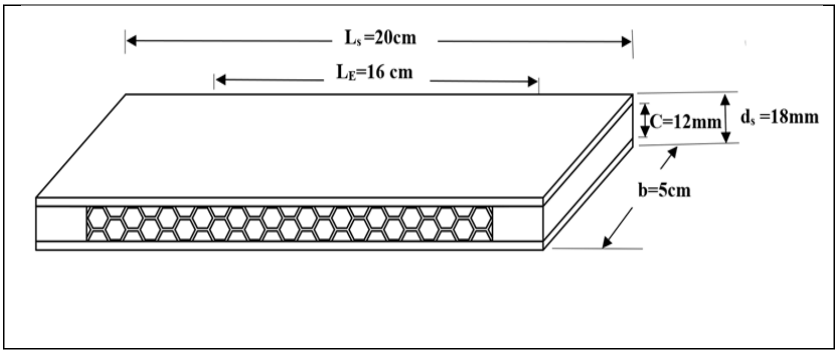

Fig. 3. Dimensions of the sandwich beam test specimen

4. VIBRATION TEST

This test was conducted in the laboratories of the mechanical department of engineering collage at the university of Kufa. All specimens were tested in accordance with (ASTM C 393-00. The following devices were employed in the experiment as shown in Fig.4:

1. Fixing stand and spacemen.
2. Accelerometer Part model (SN 151779).
3. Digital storage oscilloscope, model ADS 1202CL+ and the serial No.01020200300012.
4. Impact Hammer Instrument, model (086C03) (PCB Piezotronics vibration division), was used to exert impulse force on the cantilever beam during the transient test.
5. Model 480E09 amplifiers, which monitor the accelerometer's reaction signal and output signal to the digital storage oscilloscope.
6. Output data saved to removable disk by the oscilloscope.

Two cases of vibration examination's boundary conditions were performed Clamped-Clamped and Simply Supported, as shown in Figs. 5 and 6, respectively. In both cases, the specimens were fixed from both sides using a work clamping device, taking a distance of 2 cm from each end, so that the effective length of the specimen remained about 16 cm. Using the impulse hammer, the specimen is struck from the middle to cause vibrations, and the results that appear on the oscilloscope are recorded and saved. After completing the vibration examination procedure on all specimens, the results are processed using the (Sig-View) program and using the Fast Fourier Transform (FFT) technique. FFT converts the time response domain into the frequency response domain. The value of the maximum amplitude in the frequency response domain represents the value of the natural frequency of the beam made from composite material. The experiment was repeated three times for every type of specimen, and the average value was taken into account.

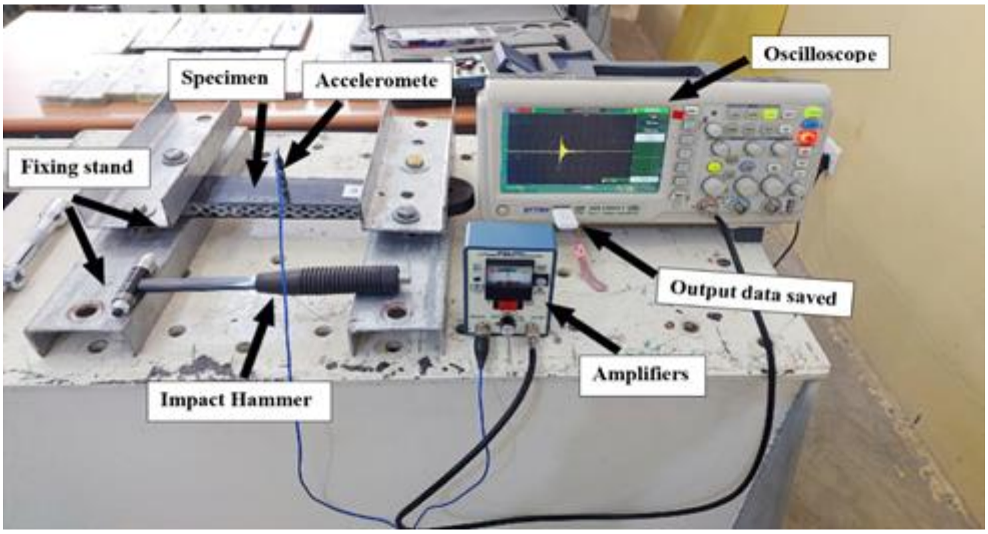

Fig. 4. the devices used for the mechanical vibration test

Fig. 5. Clamped-Clamped boundary condition

Fig. 6. Simply supported boundary condition

5. NUMERICAL ANALYSIS

The ANSYS Vibration Analysis was done through the following steps:

1. The specimen was drawn with the required dimensions using the AutoCAD program in three dimensions initially, and then it was exported to the ANSYS program.

2. The material properties for core, face sheet, and resin should be entered as shown in Figs. 7,8 and 9, which include density, Poisson's ratio, and elasticity modulus.

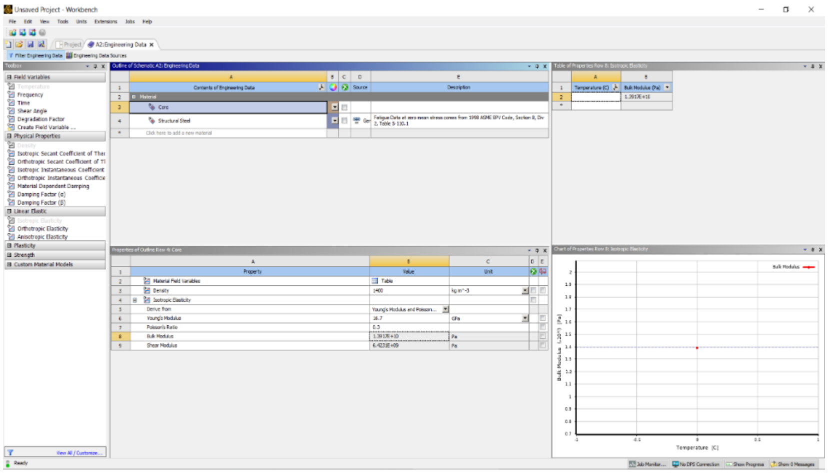

Fig. 7. Entering the material properties for the core region

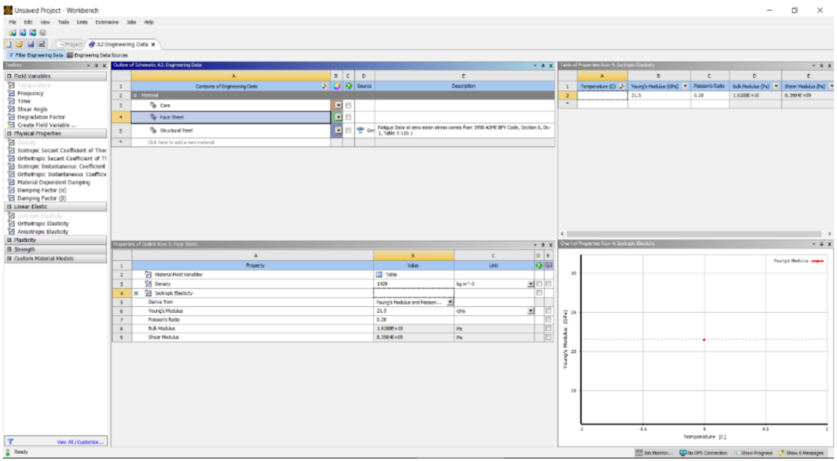

Fig. 8 Entering the material properties for face sheets regions

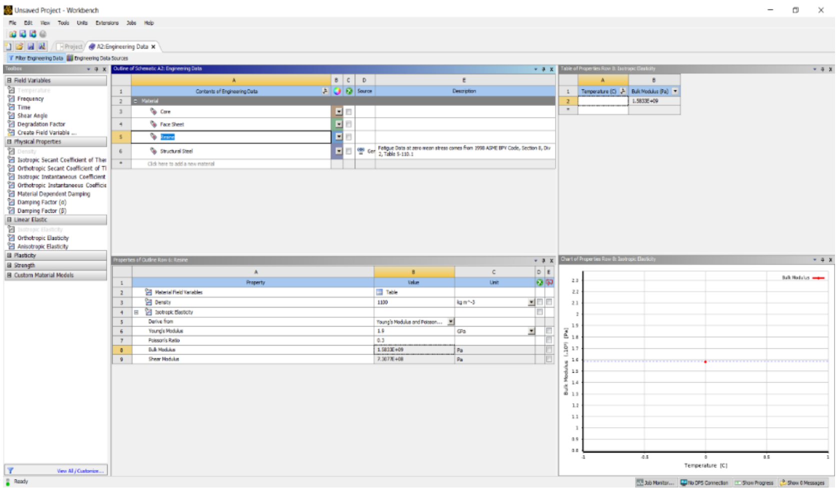

Fig. 9. Entering the material properties for the fixing or resin region

4. Set the Model
5. The used element type is (Hexahedral element) because it produces more accurate results in problems with sharp corners or edges
6. Generate Mesh
7. Select the number of modes from analysis setting
8. Apply boundary conditions of edges beam (Select outer surface of edges) as shown in Fig.10.

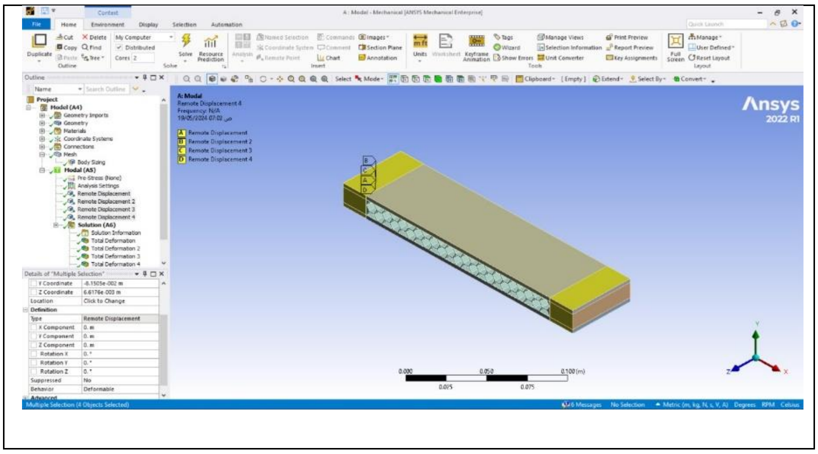

Fig. 10. Applying the boundary conditions of edges beam

9. Solve the model to get the results
10. Results total deformation with the first mode shape (Mode 1) as shown in Fig. 11 for the vibration in the same direction of the applied load.

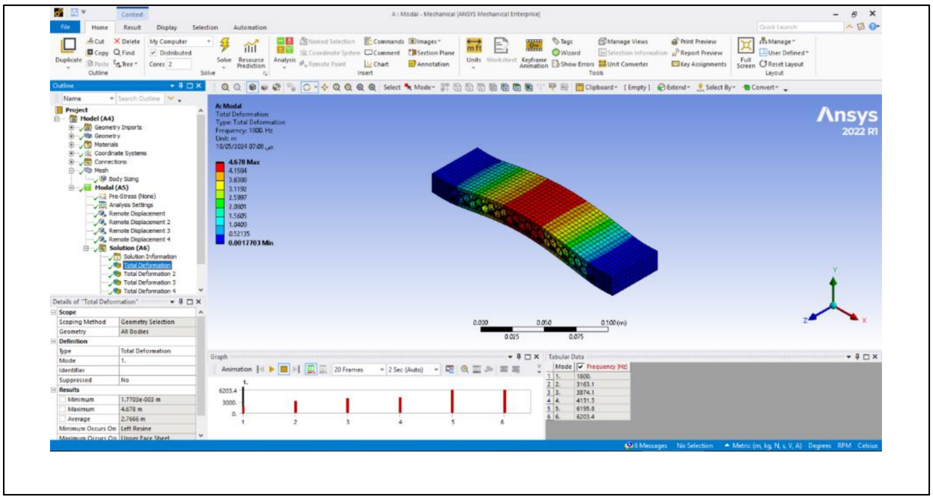

Fig. 11. The results of the total deformation with the first mode shape

6. RESULTS AND DISCUSSION

The vibration test was performed on the specimens to obtain the natural frequency values. Fig.12 shows the response-time diagram obtained by the test instrument, and Fig. 13 shows the frequency diagram obtained by using Fourier transformation in (Sig-View) software.

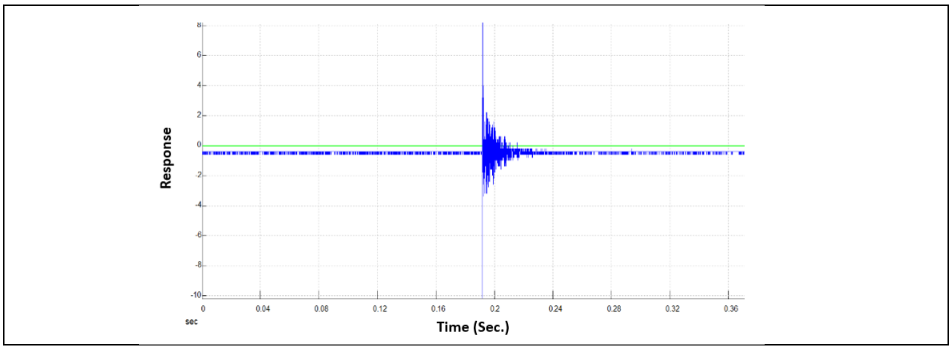

Fig.12. the response -time diagram of Specimen E4 (Clamped-Clamped)

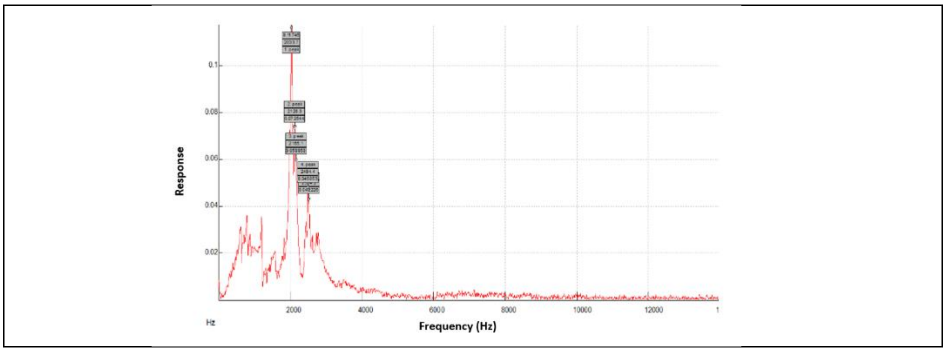

Fig. 13. The frequency diagram of specimen E4 (Clamped-Clamped)

6.1. **C**lamped-Clamped

Fig.14 represents an explanation of the relationship between natural frequency and volume fraction using the ANSYS software. It is generally observed that the natural frequency increase with the increase in volume fraction for all types of fibers used, but glass fibers achieved the least increase, followed by hybrid fibers then carbon fibers achieved the highest increase, and this applies to Fig.15 experimentally. The reason for the increase in natural frequency is due to the increase in Young's modulus.

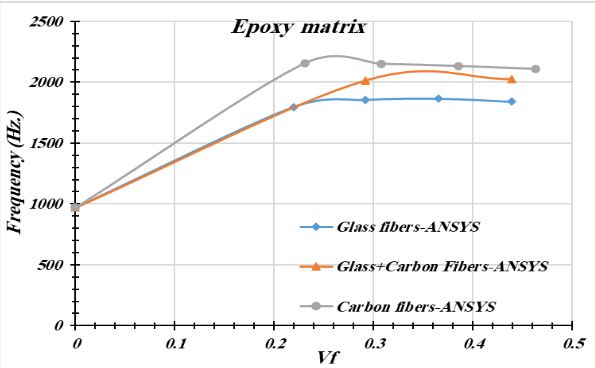

Fig.14. The natural frequency for different types of fibers with epoxy resin using ANSYS software

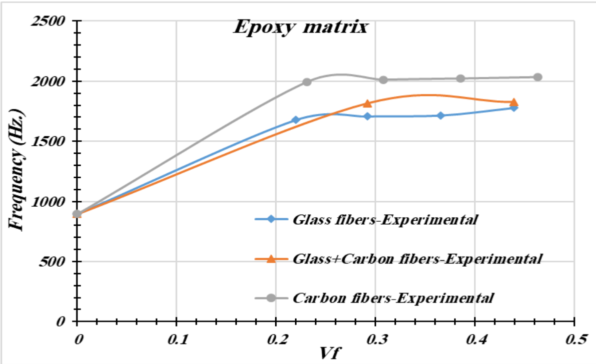

Fig.15. The natural frequency for different types of fibers with epoxy resin experimentally

As for Figs.16,17, and 18, the relationship between the natural frequency and the volume fraction of specimens filled with epoxy matrix is explained experimentally and numerically, and in three cases: once using glass fibers, once using carbon fibers, and once using hybrid fibers. In the three cases, it was observed that the natural frequency increased with the increment of volume fraction, experimentally and numerically, with an acceptable discrepancy. This increase is due to the increment of the elasticity modulus.

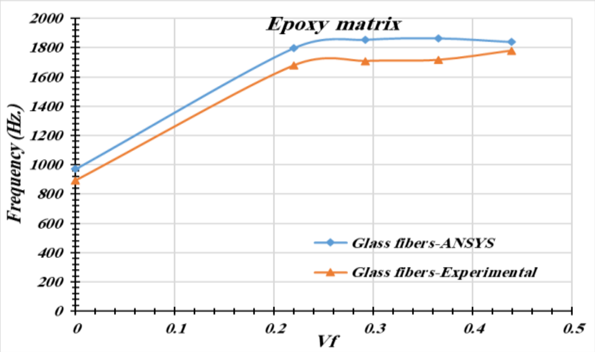

Fig. 16. The natural frequency in glass fibers with epoxy resin in both experimental and ANSYS software

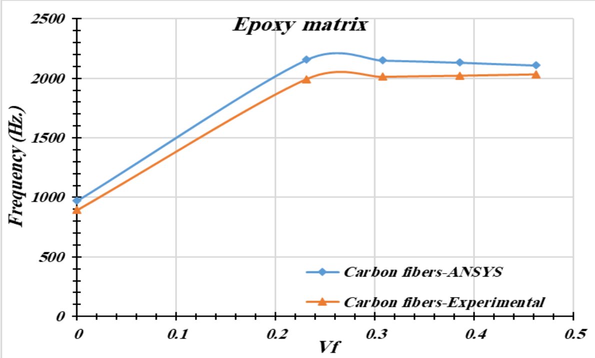

Fig.17. The natural frequency in carbon fibers with epoxy resin in both experimental and ANSYS software

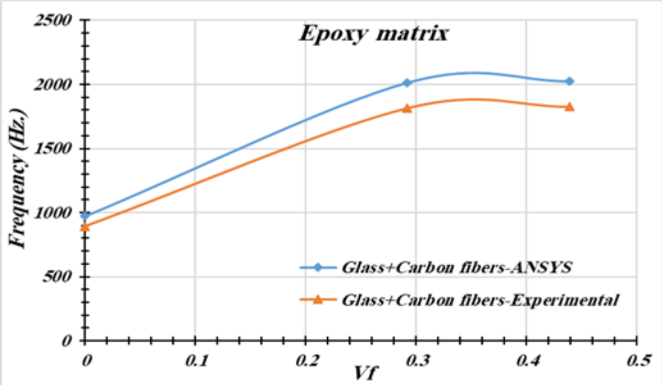

Fig. 18. The natural frequency for hybrid fibers with epoxy resin in both experimental and ANSYS software

Figs.19 and 20 represent the relationship between the natural frequency and the volume fraction for specimens filled with polyester resin for different types of fibers experimentally and using the ANSYS software. It was also observed that the natural frequency increased with increasing volume fraction for all specimens, but glass fibers achieved the lowest increase, followed by hybrid fibers, and carbon fibers achieved the highest increase. The reason for the increase in natural frequency is due to the increase in the Young's modulus.

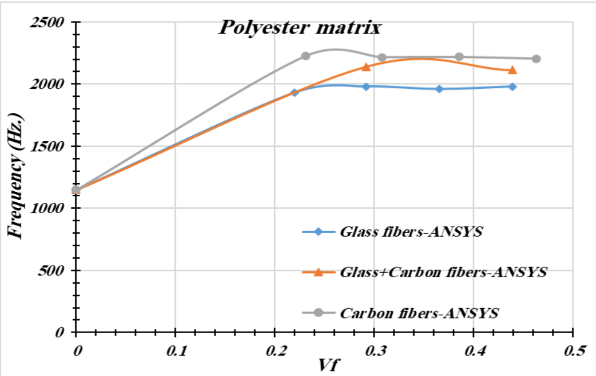

Fig.19. The natural frequency for different types of fibers with polyester resin using ANSYS software

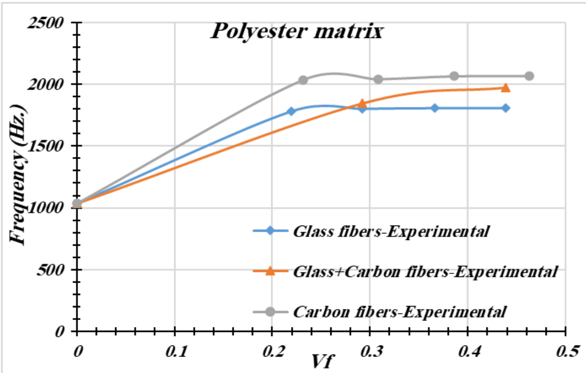

Fig.20. The natural frequency for different types of fibers with polyester resin experimentally

Figs.21,22, and 23 indicated the connection between the natural frequency and the volume fraction for specimens filled with polyester matrix experimentally, and using the ANSYS software, and in three cases: using glass fibers, using carbon fibers, and using hybrid fibers. In all types of fibers used, the natural frequency increased with increasing volume fraction due to the increase in the modulus of elasticity.

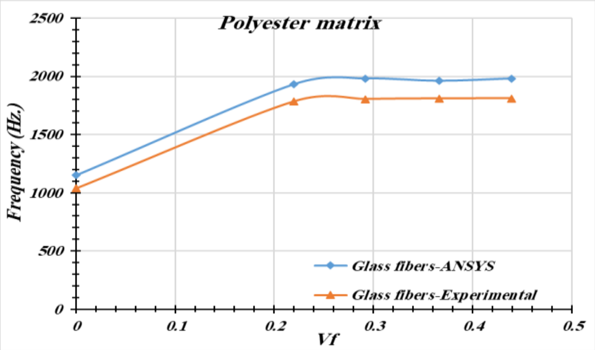

Fig.21. The natural frequency for glass fibers with polyester resin in both experimental and ANSYS software

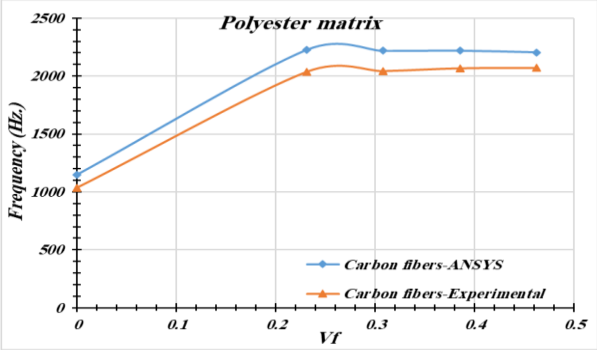

Fig.22. The natural frequency for carbon fibers with polyester resin in both experimental and ANSYS software

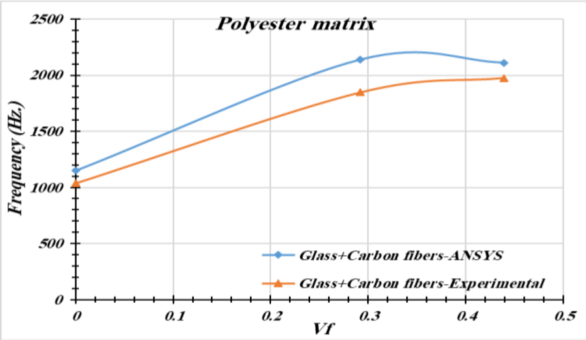

Fig. 23. The natural frequency for hybrid fibers with polyester resin in both experimental and ANSYS software

Fig.24, 25 and 26 represent the relationship between natural frequency and volume fraction. The effect of polyester matrix and epoxy matrix was compared in three cases, when the fibers used were glass fibers, when the fibers used were carbon fibers, and when the fibers used were hybrid fibers, using the ANSYS software, it was noted that the polyester matrix in all types of fibers used achieved an increase in the natural frequency higher than epoxy matrix. The explanation for this is that when the volume fraction increases, the polyester matrix achieves a higher increase in the natural frequency compared to the epoxy resin matrix due to the higher modulus of elasticity of polyester matrix as compared to epoxy matrix.

Figs.27,28 and 29 represent the connection between volume fraction and natural frequency. The effect of polyester matrix and epoxy on the specimens was compared in three cases: using glass fibers, using carbon fibers, and using hybrid fibers experimentally. It was observed in all cases that the polyester matrix had a greater effect in increasing the natural frequency than the epoxy matrix for the same previous reason.

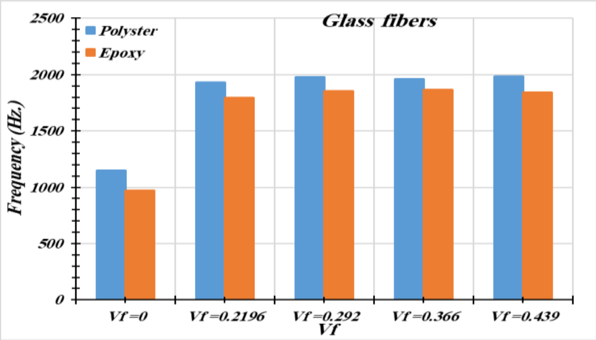

Fig. 24. Comparison of the natural frequency of glass fibers with each other using ANSYS software

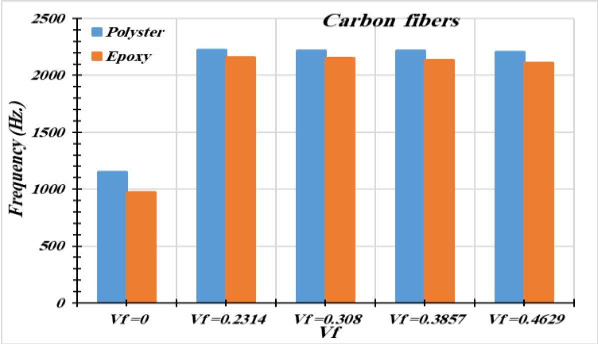

Fig. 25 Comparison of the natural frequency of carbon fibers with each other using ANSYS software

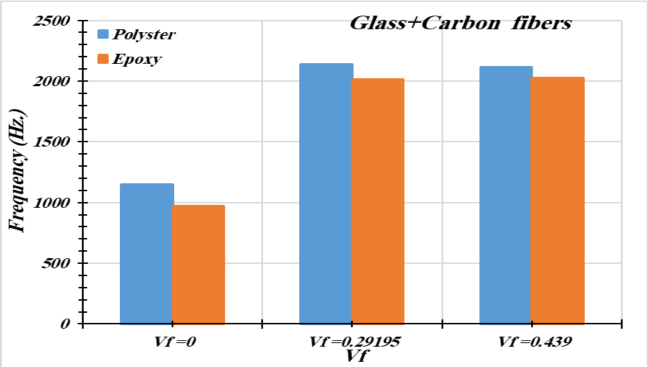

Fig.26. Comparison of the natural frequency of hybrid fibers with each other using ANSYS software

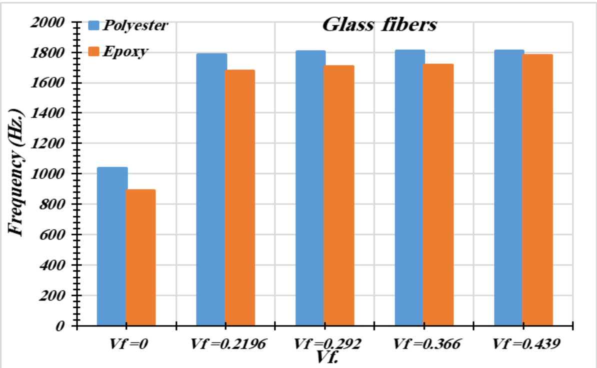

Fig. 27. Comparison of the natural frequency of glass fibers with each other experimentally

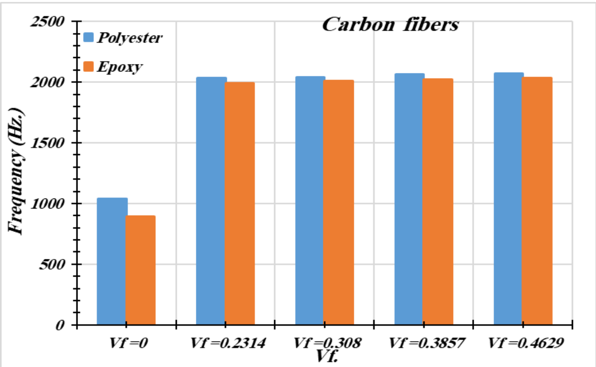

Fig.28. Comparison of the natural frequency of carbon fibers with each other experimentally

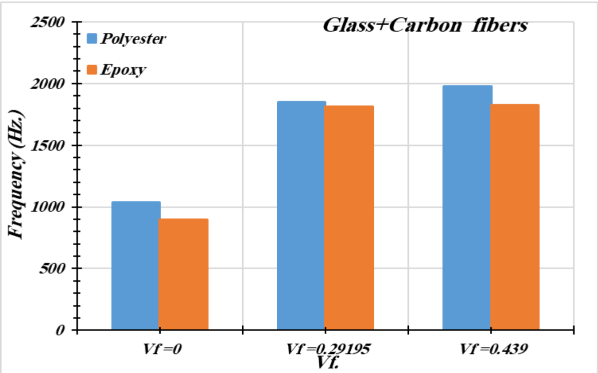

Fig.29. Comparison of the natural frequency of hybrid fibers with each other experimentally

6.2. Simply-Supported results

Figs.30 and 31 show the relationship between the natural frequency and the volume fraction for specimens filled with epoxy matrix. The comparison between the three types of fibers was done experimentally and using the ANSYS software. In both cases, the natural frequency was shown to increase with increasing volume fraction, and glass fibers achieved the least increase, then hybrid fibers and carbon fibers achieved the highest increase. The reason for the increase in natural frequency is due to the increase in Young's modulus).

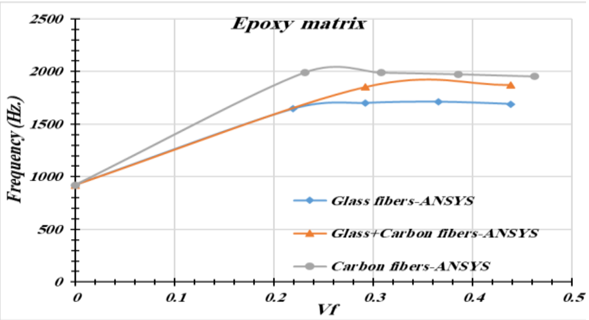

Fig.30. The natural frequency for different types of fibers with epoxy resin using ANSYS

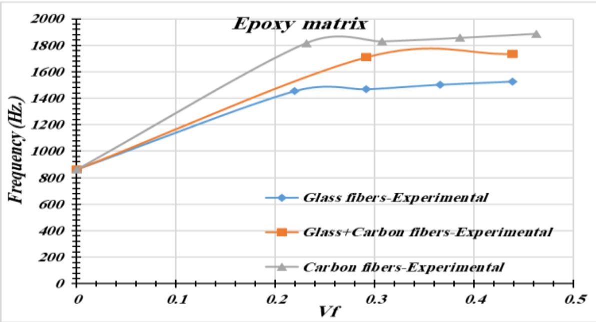

Fig.31. The natural frequency for different types of fibers with epoxy resin experimentally

Figs 32, 33, and 34 clarify the relationship between the natural frequency and the volume fraction for specimens filled with epoxy matrix experimentally and numerically. In three cases, using glass fibers, carbon fibers, and hybrid and in the three cases it was observed that the natural frequency increment with the volume fraction increment with acceptable discrepancy. This increase is due to increment of the modulus of elasticity.

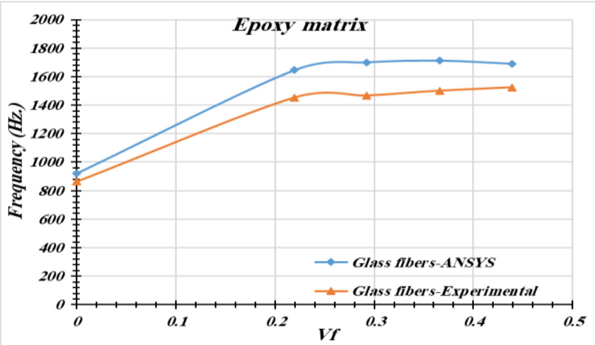

Fig. 32. The natural frequency in glass fibers with epoxy resin in both experimental and ANSYS software

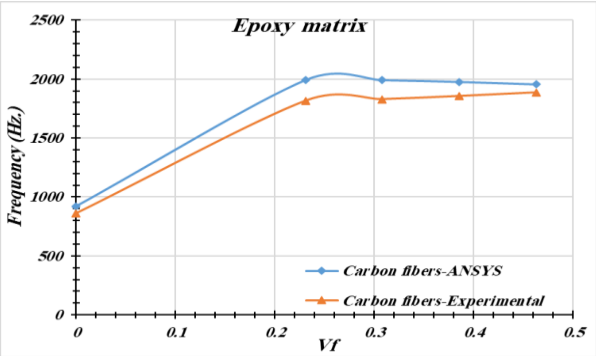

Fig 33. The natural frequency in carbon fibers with epoxy resin in both experimental and ANSYS software

Fig.35 and 36 represents the relationship between the natural frequency and the volume fraction of specimens filled with polyester resin for different types of fibers experimentally and using the ANSYS software. It was also observed that the natural frequency increased with increasing volume fraction for all specimens. However, glass fibers achieved the lowest increase, followed by carbon fibers, and hybrid fibers achieved the highest increase. The reason for the increase in natural frequency is due to the increase in Young's modulus.

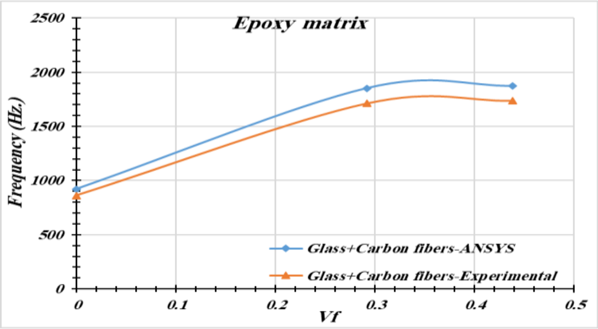

Fig.34. The natural frequency for hybrid fibers with epoxy resin in both experimental and ANSYS software

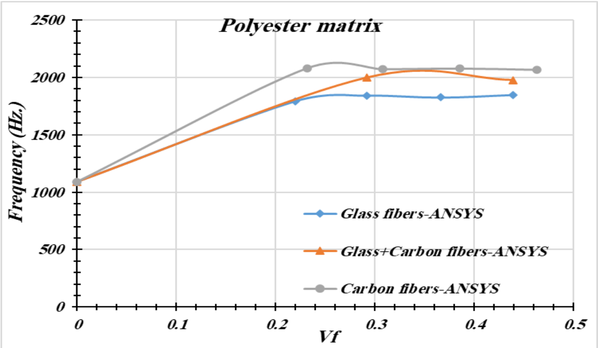

Fig.35.The natural Frequency for different types of fibers with polyester resin using ANSYS software

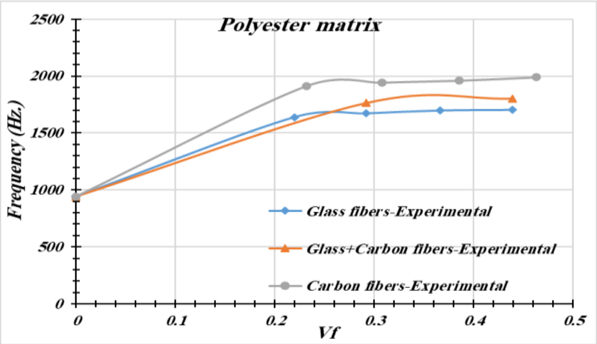

Fig.36. The natural frequency for different types of fibers with polyester resin experimentally

Figs. 37,38, and 39 represent the relationship between the natural frequency and the volume fraction of specimens filled with polyester resin experimentally, and using the ANSYS program, and in three cases: once using glass fibers, once using carbon fibers, and once using Hybrid fibers. In all types of fibers used, the natural frequency increased with increasing volume fraction. Due to an increase in the modulus of elasticity.

Figs. 40,41 and 42 represent the relationship between natural frequency and volume fraction. The effect of polyester matrix and epoxy matrix was compared in three cases, when the fibers used were glass fibers, when the fibers used were carbon fibers, and when the fibers used were hybrid fibers. Using the ANSYS software. It was noted that the polyester resin in all types of fibers used achieved a higher natural frequency increase than the epoxy resin. The explanation for this is due to the higher modulus of elasticity of polyester matrix as compared to epoxy matrix.

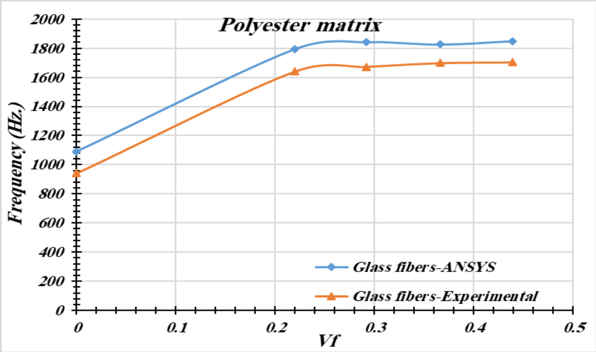

Fig. 37. The natural frequency for glass fibers with polyester resin in both experimental and ANSYS software

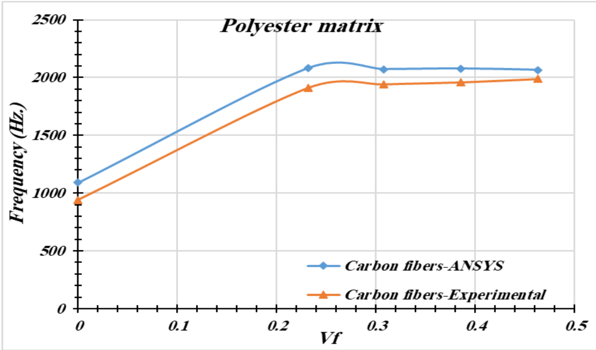

Fig. 38. The natural frequency for carbon fibers with polyester resin in both experimental and ANSYS software

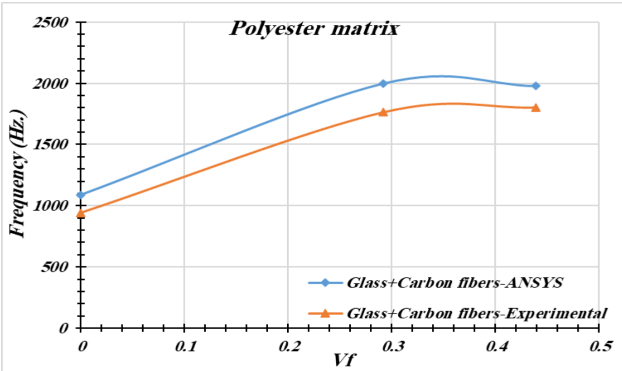

Fig. 39. The natural frequency for hybrid fibers with polyester resin in both experimental and ANSYS software

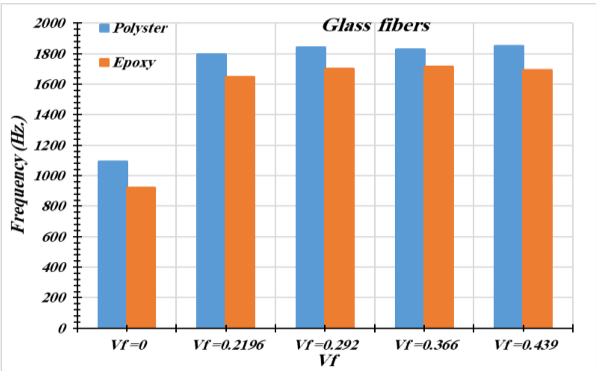

Fig. 40. Comparison of the natural frequency of glass fibers with each other using ANSYS software

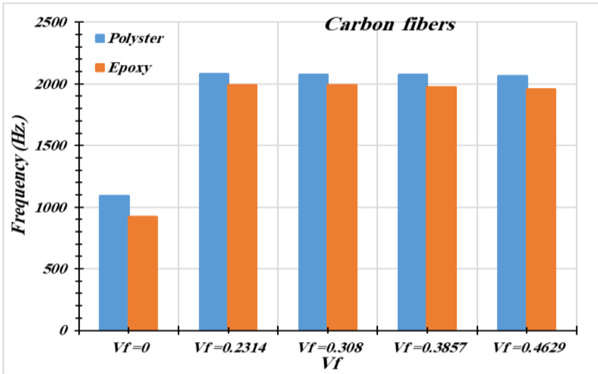

Fig. 41. Comparison of the natural frequency of carbon fibers with each other using ANSYS software

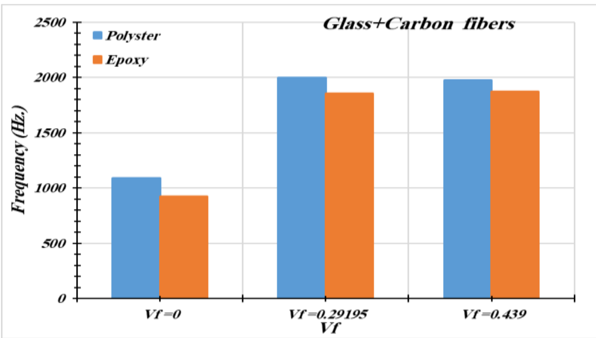

Fig. 42 Comparison of the natural frequency of hybrid fibers with each other using ANSYS software

Figs. 43, 44 and 45 represent the relationship between volume fraction and natural frequency. experimentally, the effect of polyester matrix and epoxy matrix on the specimens was compared in three cases: using glass fibers, using carbon fibers, and using hybrid. It was observed in all cases that the polyester matrix had a greater effect in increasing the natural frequency than the epoxy matrix for the same resin mentioned previously.

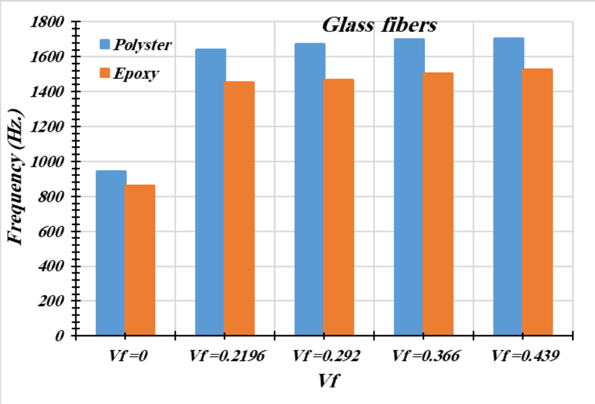

Fig. 43. Comparison of the natural frequency of glass fibers with each other experimentally

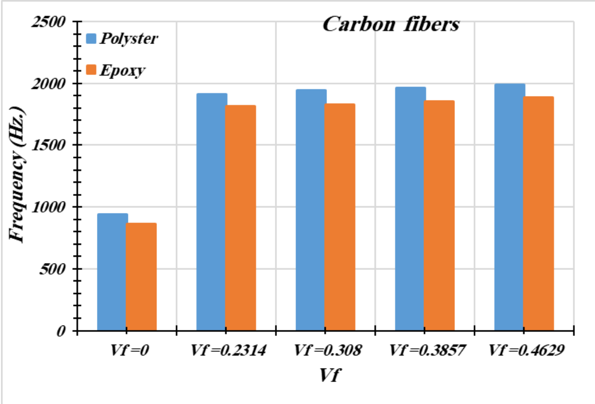

Fig. 44. Comparison of the natural frequency of carbon fibers with each other experimentally

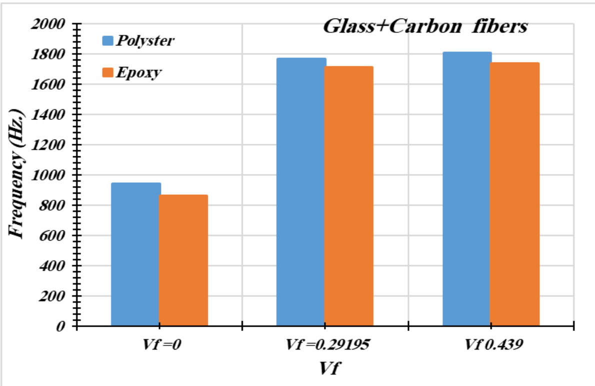

Fig. 45. Comparison of the natural frequency for hybrid fibers with each other experimentally

The final experimental and numerical results of the natural frequencies are listed in Table 6 with discrepancy between them. In Table 6, the numerical natural frequency results estimated by the ANSYS software and the experimental results under two types of boundary conditions (Clamped - Clamped) and (simply supported), were compared and a very good agreement was found. It is noted that the natural frequency values at the boundary conditions (Clamped - Clamped) are higher than the natural frequency values (simply supported), as expected because of supporting conditions.

Table 6: The numerical and experimental results of the vibration test

	Clamped-Clamped			Simply-Supported		
	Fundamental Natural Frequency (Hz)			Fundamental Natural Frequency (Hz)		
Specimen	Numerical (ANSYS)	Experimental	Discrepancy%	Numerical (ANSYS)	Experimental	Discrepancy%
A1	1796.8	1678	6.611754	1646.2	1452.9	11.74219
A2	1854.8	1709	7.860686	1701.1	1467	13.76168
A3	1864.5	1716.5	7.937785	1712.7	1501.4	12.33725
A4	1840	1779.2	3.304348	1691.5	1524.7	9.86107
B1	1931.4	1784	7.63177	1794.1	1639.7	8.605986
B2	1981.1	1804.5	8.91424	1843.1	1672.6	9.250719
B3	1961.2	1809.9	7.714664	1826.1	1698.3	6.998521
B4	1981.2	1811	8.590753	1849.3	1703.5	7.884064
C1	2012.9	1815	9.831586	1852.8	1711.9	7.604706
C2	2024.8	1826.5	9.79356	1874	1736.5	7.337247
D1	2140.4	1846.5	13.73108	1998.5	1765	11.68376
D2	2112.4	1975.1	6.499716	1977.7	1804.5	8.757648
E1	2157.6	1994.8	7.545421	1992.9	1817.3	8.81128
E2	2151.2	2013	6.424321	1990.2	1828.9	8.104713
E3	2133.1	2022.7	5.175566	1975.1	1855.8	6.0402
E4	2110	2033.7	3.616114	1954.5	1886.4	3.484267
F1	2227.2	2037	8.539871	2079.7	1911	8.111747
F2	2217.3	2042.3	7.892482	2072.5	1942.4	6.277443
F3	2219	2066.5	6.872465	2077.6	1959.8	5.670004
F4	2205.1	2069	6.172056	2066.3	1988.7	3.755505
G1	1149.2	1036.9	9.772015	1090.5	942.08	13.61027
G2	972.28	894	8.051179	921.19	862.61	6.359166

7. CONCLUSIONS

From the procedure of this study, the following conclusions can be obtained:

1. At the boundary conditions (clamped - clamped), carbon fibers with polyester matrix achieved the highest increase in the natural frequency value, which reached (2069 Hz) experimentally and (2205.1 Hz) numerically at the volume fraction (46.288%). When using the epoxy matrix, carbon fibers achieved the highest increase in the natural frequency value, which reached (2033.7 Hz) experimentally and (2110 Hz) numerically at the volume fraction (46.288%).

2. Under the simply supported boundary conditions, carbon fibers with polyester matrix achieved the highest increase in the natural frequency value, which reached (1988.7 Hz) experimentally and (2066.3 Hz) numerically at the volume fraction (46.288%). When using epoxy matrix, carbon fibers achieved the highest increase in the natural frequency value, which reached (1886.4 Hz) experimentally and (1954.5 Hz) numerically at the volume fraction (46.288%).

3. There was a very good agreement reached between the numerical natural frequency results estimated by the ANSYS software and the experimental results under two types of boundary conditions (fixed-fixed) and (simply supported). The highest error rate in (Clamped-Clamped) boundary condition about (13.73108%) and in (Simply supported) boundary conditions (13.76168 %).
4. The natural frequency values at the boundary conditions (Clamped - Clamped) are higher than the natural frequency values (simply supported) because of supporting conditions.

8. REFERENCES

A. Elmushyakhi, "Collapse mechanisms of out-of-plane preload composite sandwich beams under in-plane loading," Journal of Building Engineering, vol. 26, p. 100875, 2019.

A. Monti, A. El Mahi, Z. Jendli, and L. Guillaumat, "Experimental and finite elements analysis of the vibration behaviour of a bio-based composite sandwich beam," Composites Part B: Engineering, vol. 110, pp. 466-475, 2017.

B. Safaei et al., "Free vibration investigation on RVE of proposed honeycomb sandwich beam and material selection optimization," vol. 21, no. 1, pp. 031-050, 2023.

C.-D. Chen and P.-W. J. A. M. Su, "An analytical solution for vibration in a functionally graded sandwich beam by using the refined zigzag theory," vol. 232, pp. 4645-4668, 2021.

D. Chen, S. Kitipornchai, and J. Yang, "Nonlinear free vibration of shear deformable sandwich beam with a functionally graded porous core," Thin-Walled Structures, vol. 107, pp. 39-48, 2016.

D. K. Nguyen, A. N. T. Vu, N. A. T. Le, V. N. J. S. Pham, and vibration, "Dynamic behavior of a bidirectional functionally graded sandwich beam under nonuniform motion of a moving load," vol. 2020, pp. 1-15, 2020.

E. F. Erdurcan and Y. Cunedioğlu, "Free vibration analysis of a functionally graded material coated aluminum beam," AIAA Journal, vol. 58, no. 2, pp. 949-954, 2020.

E. Taati and F. Fallah, "Exact solution for frequency response of sandwich microbeams with functionally graded cores," Journal of Vibration and Control, vol. 25, no. 19-20, pp. 2641-2655, 2019.

F. de Souza Eloy, G. F. Gomes, A. C. Ancelotti Jr, S. S. da Cunha Jr, A. J. F. Bombard, and D. M. Junqueira, "Experimental dynamic analysis of composite sandwich beams with magnetorheological honeycomb core," Engineering Structures, vol. 176, pp. 231-242, 2018.

F. Ebrahimi and N. Farazmandnia, "Thermo-mechanical vibration analysis of sandwich beams with functionally graded carbon nanotube-reinforced composite face sheets based on a higher-order shear deformation beam theory," Mechanics of Advanced Materials and Structures, vol. 24, no. 10, pp. 820-829, 2017.

F. Ebrahimi and N. Farazmandnia, "Vibration analysis of functionally graded carbon nanotube-reinforced composite sandwich beams in thermal environment," Advances in aircraft and spacecraft science, vol. 5, no. 1, p. 107, 2018.

F. Ebrahimi, N. J. A. i. a. Farazmandnia, and s. science, "Vibration analysis of functionally graded carbon nanotube-reinforced composite sandwich beams in thermal environment," vol. 5, no. 1, p. 107, 2018.

F. Ebrahimi, N. J. M. o. A. M. Farazmandnia, and Structures, "Thermo-mechanical vibration analysis of sandwich beams with functionally graded carbon nanotube-reinforced composite face sheets based on a higher-order shear deformation beam theory," vol. 24, no. 10, pp. 820-829, 2017.

F. T. C. L. https: //utekcomposites. en. made-inchina. com/product/souJDNZCGFrM/Chin.-H.-S.-600GSM-F.-W.-R. html. Product Data Sheet, ed.

H. A. C. M. C. L. http://www. anjiezj. com/en/en/ProductShow. asp?ID=70. Product Data Sheet, “No Title.”, ed.

H. Liu, Z. Lv, and H. J. C. S. Wu, "Nonlinear free vibration of geometrically imperfect functionally graded sandwich nanobeams based on nonlocal strain gradient theory," vol. 214, pp. 47-61, 2019.

I. c. r. C. L. "Technical Data Sheet" , Dammam, Saudi Arabia., ed.

J. Liu, C. Hao, Y. Zhou, and W. J. E. A. w. B. E. Ye, "Dynamic analysis of functionally graded sandwich beams using a semi-analytic method named scaled boundary finite element method," vol. 130, pp. 161-175, 2021.

J. Liu, C. Hao, Y. Zhou, and W. Ye, "Dynamic analysis of functionally graded sandwich beams using a semi-analytic method named scaled boundary finite element method," Engineering Analysis with Boundary Elements, vol. 130, pp. 161-175, 2021.

K. Alambeigi, M. Mohammadimehr, M. Bamdad, and T. J. A. M. Rabczuk, "Free and forced vibration analysis of a sandwich beam considering porous core and SMA hybrid composite face layers on Vlasov’s foundation," vol. 231, pp. 3199-3218, 2020.

L. Liu, W. Yang, Y. Chai, and G. J. A. o. A. M. Zhai, "Vibration and thermal buckling analyses of multi-span composite lattice sandwich beams," vol. 91, pp. 2601-2616, 2021.

L. Xin and Y. Kiani, "Vibration characteristics of arbitrary thick sandwich beam with metal foam core resting on elastic medium," in Structures, 2023, vol. 49, pp. 1-11: Elsevier.

M. Avcar, L. Hadji, and Ö. Civalek, "Natural frequency analysis of sigmoid functionally graded sandwich beams in the framework of high order shear deformation theory," Composite Structures, vol. 276, p. 114564, 2021.

M. Momeni, M. B. J. M. o. A. M. Dehkordi, and Structures, "Frequency analysis of sandwich beam with FG carbon nanotubes face sheets and flexible core using high-order element," vol. 26, no. 9, pp. 805-815, 2019.

M. S. Nematollahi, H. Mohammadi, R. Dimitri, and F. J. A. S. Tornabene, "Nonlinear vibration of functionally graded graphene nanoplatelets polymer nanocomposite sandwich beams," vol. 10, no. 16, p. 5669, 2020.

M. Subramani, S. Rajeshkumar, and M. J. M. T. P. Ramamoorthy, "Free vibration analysis of the MWCNT reinforced hybrid laminated composite sandwich beam," vol. 22, pp. 3220-3225, 2020.

N. T. 2021 Data sheet of Epoxy resin (Renksan - Renfloor HT 2000)/ USA, ed.

N. Thanikasalam and M. J. P. C. Ramamoorthy, "Free and forced vibration response of a laminated composite sandwich beam with dual honeycomb core: numerical and experimental study," vol. 44, no. 8, pp. 5214-5231, 2023.

P. Li, K. Wang, and B. J. T.-W. S. Wang, "Nonlinear vibration of the sandwich beam with auxetic honeycomb core under thermal shock," vol. 196, p. 111479, 2024.

Q. Lu, P. Wang, and C. J. I. J. o. M. S. Liu, "An analytical and experimental study on adaptive active vibration control of sandwich beam," vol. 232, p. 107634, 2022.

R. Selvaraj and M. Ramamoorthy, "Dynamic analysis of laminated composite sandwich beam containing carbon nanotubes reinforced magnetorheological elastomer," Journal of Sandwich Structures & Materials, vol. 23, no. 5, pp. 1784-1807, 2021.

R. Selvaraj, K. Gupta, S. K. Singh, A. Patel, M. J. P. Ramamoorthy, and P. Composites, "Free vibration characteristics of multi-core sandwich composite beams: experimental and numerical investigation," vol. 29, no. 9_suppl, pp. S1414-S1423, 2021.

R. Selvaraj, M. J. J. o. S. S. Ramamoorthy, and Materials, "Dynamic analysis of laminated composite sandwich beam containing carbon nanotubes reinforced magnetorheological elastomer," vol. 23, no. 5, pp. 1784-1807, 2021.

R. Selvaraj, M. Subramani, G. More, and M. J. M. T. P. Ramamoorthy, "Dynamic responses of laminated composite sandwich beam with double-viscoelastic core layers," vol. 46, pp. 7468-7472, 2021.

S. Bakhy, M. Al-Waily, and M. Al-Shammari, "Analytical and numerical investigation of the free vibration of functionally graded materials sandwich beams," Archives of Materials Science and Engineering, vol. 110, no. 2, 2021.

S. Bakhy, M. Al-Waily, M. J. A. o. M. S. Al-Shammari, and Engineering, "Analytical and numerical investigation of the free vibration of functionally graded materials sandwich beams," vol. 110, no. 2, 2021.

S. J. A. J. Yildirim, "Free vibration analysis of sandwich beams with functionally-graded-cores by complementary functions method," vol. 58, no. 12, pp. 5431-5439, 2020.

S. M. Marandi and I. J. E. S. Karimipour, "Free vibration analysis of a nanoscale FG-CNTRCs sandwich beam with flexible core: Implementing an extended high order approach," vol. 276, p. 115320, 2023.

T. A. Aslan, A. R. Noori, and B. Temel, "An efficient approach for free vibration analysis of functionally graded sandwich beams of variable cross-section," in Structures, 2023, vol. 58, p. 105397: Elsevier.

V. Gopalan, V. Suthenthiraveerappa, S. K. Tiwari, N. Mehta, and S. J. E. M. R. Shukla, "Dynamic characteristics of a honeycomb sandwich beam made with jute/epoxy composite skin," vol. 9, no. 1, pp. 132-140, 2020.

V. Gopalan, V. Suthenthiraveerappa, S. K. Tiwari, N. Mehta, and S. Shukla, "Dynamic characteristics of a honeycomb sandwich beam made with jute/epoxy composite skin," Emerging Materials Research, vol. 9, no. 1, pp. 132-140, 2020.